Fundamentals of Discharge Initiation in Pulsed Plasma Thrusters: Threshold Criteria for Undervoltage Breakdown

IEPC-2007-237

Presented at the 30th International Electric Propulsion Conference, Florence, Italy
September 17-20, 2007

James E. Cooley* and Edgar Y. Choueiri†
Princeton University, Princeton, NJ, 08544, USA

In an effort to understand the basic mechanism behind discharge initiation in gas-fed pulsed plasma thsuters, the conditions under which an externally supplied pulse of electrons will induce breakdown in an undervoltaged, low-gain discharge gap are experimentally and theoretically explored. The minimum number of injected electrons required to achieve breakdown in a parallel-plate gap is measured in argon at pd values of 3-10 Torr-m using ultraviolet laser pulses to photoelectrically release electrons from the cathode. This value was found to scale inversely with pressure and voltage. A dimensionless theoretical description of the phenomenon is formulated and numerically solved. It is determined that Townsend's classic breakdown condition, $\mu > 1$, is a necessary but not sufficient condition to achieve breakdown at an undervoltage. Instead, it is found that a significant fraction of the charge on the plates must be injected for breakdown to be achieved at low gain. It is also found that fewer electrons are required as the gain due to electron-impact ionization (α process) is increased, or as the sensitivity of the α process to electric field is enhanced by increasing gas pressure. A predicted insensitivity to ion mobility implies that breakdown is determined during the first electron avalanche when space charge distortion is greatest.

*Graduate Research Assistant, Mechanical and Aerospace Engineering Department, cooley@princeton.edu.
†Chief Scientist, EPPDyL. Associate Professor, Mechanical and Aerospace Engineering Department. Associated Faculty, PPPL. choueiri@princeton.edu.

Nomenclature

A = empirical coefficient for determining α
α = first Townsend ionization coefficient
B = empirical coefficient for determining α
d = gap width
E = electric field
ϕ = electrostatic potential
γ = secondary emission coefficient
$\Gamma_{e,+}$ = electron, ion flux
μ = breakdown parameter
$\mu_{e,+}$ = electron, ion mobility
$n_{e,+}$ = electron, ion density
N_{e0} = injected electron pulse areal density
$\bar{N}^*_{e0}$ = threshold dimensionless pulse density
ν = Courant number
p = gas pressure
q' = reference variable
$\bar{q}$ = normalized variable
t = time
τ = temporal width of the injected electron pulse
$v_{e,+}$ = electron, ion velocity
V = applied electrode voltage
V_b = breakdown voltage
x = position coordinate
ξ = ion avalanche time coordinate

I. Introduction

UNDERVOLTAGE breakdown is the phenomenon in which a burst of electrons at the cathode of a discharge gap that is held below its breakdown voltage leads to a discharge. It is the fundamental mechanism employed by discharge initiation systems for gas-fed pulsed plasma thrusters (GFPPTs),[1] which usually use sparkplugs as the source of the triggering pulse. Sparkplugs, however, erode with each firing and limit thruster lifetime. Other discharge initiation systems have been proposed[2] using, for example, photoelectric electron sources, but any successful discharge initiation system will likely rely on undervoltage breakdown.[3]

The phenomenon was first observed experimentally by Kluckow[4] as reported by Raether.[5] Work was carried out by others,[6,7] most extensively Sato and Sakamoto who investigated the phenomenon in air, theoretically and experimentally, over a range of pressures. Fonte[8] modeled breakdown of parallel-plate avalanche chambers and showed that the breakdown threshold — the minimum criteria under which breakdown will occur in those devices, corresponds to the conditions necessary for streamer formation — as predicted by Raether.[5] This result is consistent with experimental measurements of breakdown threshold in parallel-plate avalanche chambers for a variety of conditions.[9]

That work described well the breakdown behavior in such high-gain ($e^{\alpha_0 d}$ greater than about 10^4) devices in which streamer formation is the dominant breakdown mechanism. However, the literature contains numerous examples of undervoltage breakdown through a Townsend-like, or "slow" breakdown mechanism at lower gain, in which breakdown is achieved through the buildup of successively larger generations of avalanches enhanced by space charge effects. Yet, no discussion of threshold criteria for such a phenomenon has been reported. Since GFPPTs typically operate at low pressure (on the order of 1 mTorr) and low voltage (on the order of 100 V), they are inherently low-gain devices. Understanding threshold criteria for undervoltage breakdown at low-gain is therefore our primary focus in this work — we will both experimentally measure and theoretically calculate the critical injected charge required to achieve breakdown in an undervoltaged discharge gap, and explore the dependencies of this value on relevant experimental parameters so as to achieve a fundamental understanding of the physical mechanisms that govern this phenomenon.

In Section II, we present the results of an experiment designed to measure the critical charge required for undervoltage breakdown. The discharge is achieved in a parallel-plate discharge gap through the injection of electron pulses resulting from laser pulses directed onto a photo-emissive target fixed to the cathode. Argon is used at relatively low pressure (on the order of 1 Torr) and the experimentally observed breakdown timescale implies the prominence of the Townsend mechanism.

Section III contains a formulation of a dimensionless theoretical description of undervoltage breakdown. The primary aim of this theoretical work is to find the simplest model that explains the observed experimental trends in critical injected density. As such, we make a number of simplifying assumptions that allow us to clarify the most relevant mechanisms at work in our experimental arrangement. We then explore, to the extent that those assumptions hold, the dependencies of this value on various parameters (gas pressure, voltage, gap width, ion mobility, secondary emission coefficient).

Finally, in Section IV, we will discuss a number of physical insights gleaned from examination of the experimental and theoretical results.

II. Experiment

The experiment is designed to measure the minimum injected charge required to achieve undervoltage breakdown for a given set of initial conditions. Intended to be as simple as possible for phenomenological clarity, the apparatus is a parallel-plate discharge gap and argon is used as the working gas.

A. Experimental Setup and Methods

Figure 1 is a schematic of the experimental setup. A pulsed laser is directed through a beamsplitter which reflects a small fraction (approximately 1 %) of the beam onto a photodiode. We use a Q-switched Nd:YAG it its fourth harmonic of 266 nm, a pulse width of 10 ns, and a maximum energy of 4 mJ — not enough to significantly heat the surface so that electron emission is presumed to result from the photoelectric effect. The beam passes through the window of a vacuum chamber and onto an OFHC copper target fixed to the cathode of a pair of parallel-plate electrodes, separated by a gap width of 2.54 cm. The chamber is evacuated to a pressure of 10^{-9} Torr, then filled with argon to the desired pressure, ranging from 1-3 Torr. A voltage-regulated power supply maintains a static potential across the electrodes, which float with respect to ground.

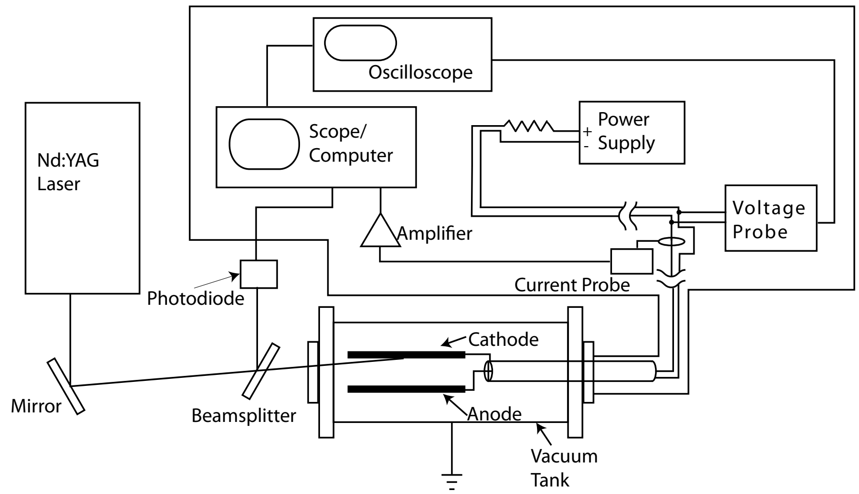

Figure 1. Schematic of the undervoltage breakdown experiment.

Current signals are carried out from the plates by way of a 50Ω transmission line and are measured by an inductive current transformer, whose signal is amplified and recorded on a Tektronix 5104b oscilloscope, which also measures the photodiode signal. The voltage across the plates is measured and recorded by a separate oscilloscope. All measurement electronics sit inside a grounded Faraday cage that isolates them from electromagnetic noise. The system is run by an automated Labview data acquisition system.

The breakdown voltage is measured several times to an accuracy of about 2%, then a desired undervoltage is applied across the plates. Because ionization avalanching amplifies the initial electron pulse in the presence of gas, we performed an *a priori* vacuum calibration, correlating the charge released with the intensity of the laser pulse. In the presence of gas, measurement of the laser intensity thus allowed us to calculate the initial charge released.

Figure 2 contains examples of the oscilloscope traces used to calculate the threshold curves. For each laser firing, one set of photodiode and voltage traces is recorded and analyzed. The timescales on the two traces are different; a laser pulse would appear as instantaneous at $t = 0$ on the voltage trace. The traces in Figure 2 (a) represent a relatively weak laser pulse that does not result in a breakdown; no change in voltage is observed. In (b), however, a more intense pulse does result in breakdown. This is manifested in a drop in voltage across the electrodes. Such a voltage drop always corresponds to formation of visible plasma between the electrodes. Note the timescale of the voltage drop, on the order of 10 microseconds. Such a timescale corresponds to several ion transit times (on the order of 1 μs), implying that Townsend, not streamer, breakdown is at work.

For each photodiode trace, the small DC offset is subtracted and the maximum value is recorded. The corresponding voltage trace is then analyzed to determine if a breakdown occurred. A weighted histogram is then calculated which divides the entire range of charge values into bins and specifies the fraction of shots within each bin that resulted in a breakdown.

B. Results

Such a histogram is plotted in Figure 3. Charge error bars come from the vacuum pulse calibration and represent the root mean square deviation of charges for a given photosignal bin. Error bars on the probability are calculated based on binomial error, $\sigma = \sqrt{p(1-p)/n}$ where p is the fraction of times a pulse in that charge bin caused a breakdown and n is the number of pulses in the bin.

We see that at very low values of initial charge, breakdown is very unlikely, at very high values, breakdown is very likely, and that some intermediate regime exists. The quantity we are seeking, the number of electrons (or the total charge) in a pulse required to achieve undervoltage breakdown, can be gleaned from graphs such as this.

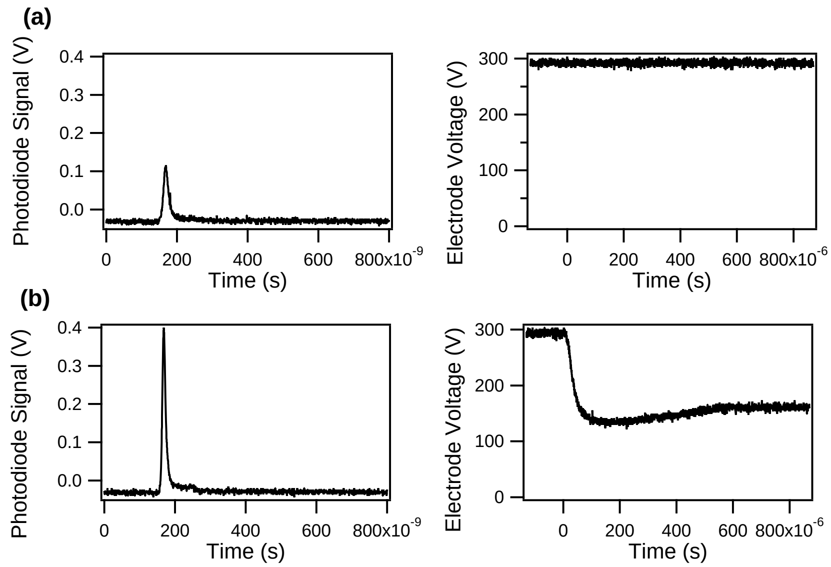

Figure 2. Two pairs of oscilloscope traces recorded in the undervoltage breakdown experiment. These were taken with argon at 3 Torr, and an initial electrode voltage of 295 V.

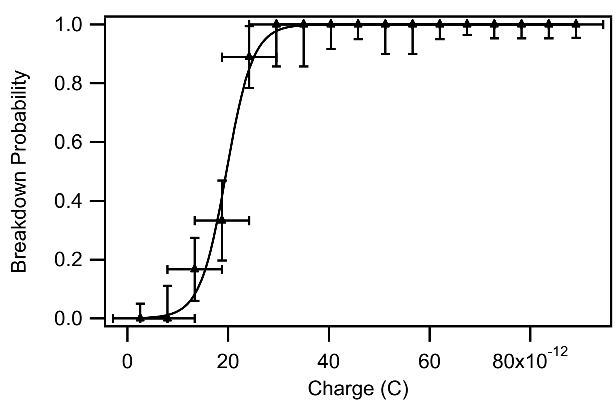

Figure 3. Probability of breakdown as a function of charge in the initial pulse for argon at 3 Torr and 295 V. A least-squares fit of Equation 1 is overlayed.

We fit the data to sigmoid functions of the form:

$$y(x) = \frac{1}{1+\exp\left(\frac{x_{1/2}-x}{\nu}\right)}, \tag{1}$$

which assumes that $y(x)$ reaches unity as $x \to \infty$ and vanishes as $x \to 0$. $x_{1/2}$ represents the charge value at which the breakdown probability is 50 %. We will define this value as the threshold charge and plot it for varied experimental conditions. Because of the steepness of the breakdown probability curves, the results are insensitive to the definition of threshold charge.

In Figure 4, we show the experimentally measured threshold charge as a function of V/V_b (plate voltage normalized to the breakdown voltage at each pressure) for argon at pressures of 1.6 Torr, 2 Torr, and 3 Torr. Error bars represent the error on the fit parameter $x_{1/2}$ from Equation 1. Least squares fits of all data sets yielded χ^2/M, where M is the number of relevant degrees of freedom, ranging from about .5 to 1.

The results demonstrate a trend of decreasing threshold charge with increasing pressure and, at least at lower pressure values, with increasing voltage. The experiment was also carried out at pressures of 1.5 Torr, 1.4 Torr, and 1 Torr, but no breakdowns occurred at these lower pressures.

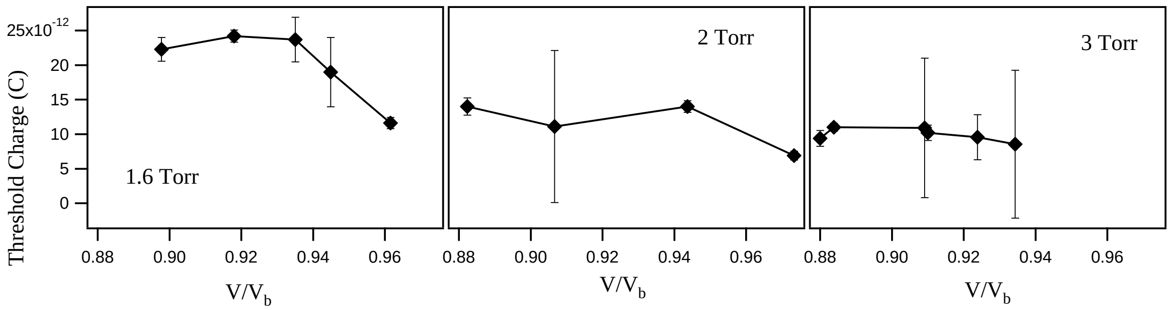

Figure 4. Threshold charge as measured by the undervoltage breakdown experiment in argon at 1.6 Torr, 2 Torr, and 3 Torr.

III. Theory

A. Formulation

We now seek to find the simplest model that demonstrates the observed experimental trends, so we treat one-dimensional discharge gaps with non-attaching gases in which secondary emission is only through ion impact and is field-independent. We also adopt the assumptions that the mobilities are field-independent and that diffusion and particle loss are negligible. Use of these assumptions allows us to describe the problem with a relatively small number of dimensionless parameters.

Of course, one could consider a variety of extensions to this model, exploring the roles of field-dependent or photon-based secondary emission, multidimensional effects, field-dependent mobilities, attachment, diffusion, loss, or nonlocal ionization rates as appropriate for a specific application. Our idealized approach in this work could thus serve as a starting point for such future efforts. In particular, we expect a field-dependent γ and photoelectric secondary emission to play large roles in undervoltage breakdown for contaminated cathodes and discharges of low E/p.

Our formulation begins with the fluid-based approach employed in the "classical model" for glow discharges that was originally presented by von Engel and Steenbeck[10] but treated by many other authors (see, for example,[5,11,12]). The governing equations are continuity equations for electrons and singly charged ions and Poisson's equation:

$$\frac{dn_e}{dt} = \alpha\Gamma_e - \frac{d}{dx}\Gamma_e \tag{2}$$

$$\frac{dn_+}{dt} = \alpha\Gamma_e + \frac{d}{dx}\Gamma_+ \tag{3}$$

$$\frac{d^2\phi}{dx^2} = \frac{-e}{\epsilon_0}(n_+ - n_e) \tag{4}$$

$$E = -\frac{d\phi}{dx}. \tag{5}$$

We assume that the velocities of electrons and ions are the drift velocities so that $\Gamma_{e,+} = n_{e,+}\mu_{e,+}E$ is the flux of each respective species. If we define $x = 0$ as the cathode position and $x = d$ as the anode, then the governing equations are subject to the boundary conditions:

$$\phi(0,t) = 0 \tag{6}$$

$$\phi(d,t) = V \tag{7}$$

$$\Gamma_e(0,t) = \gamma\Gamma_+(0,t) + \Gamma_{pulse}(t). \tag{8}$$

Equations 6 and 7 state that the potential difference across the electrodes is held at the applied voltage. Equation 8 is the boundary condition for electron flux and the cathode and includes secondary emission from the cathode from ions and photons. γ is the secondary emission coefficient from ion impact on the cathode. We neglect secondary emission due to photon impact. The cathode boundary condition treats the external pulse of electrons:

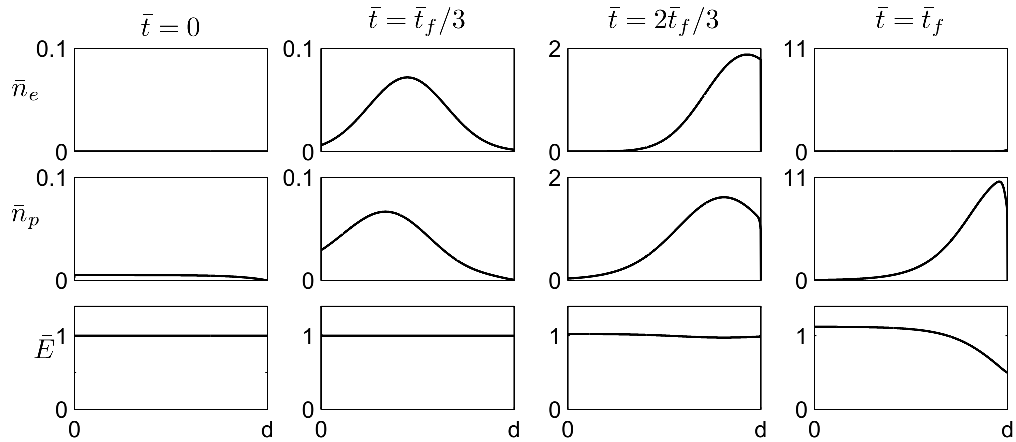

Figure 5. Time dependent variation of normalized electron density, ion density, and electric field at various times during the initial electron avalanche transit. Here $\bar{p}=2.15$, $\alpha_0 d=7$, and $\bar{N}_{e0}=4\times10^{-2}$. Note the scale changes on the density plots.

$$\Gamma_{pulse}(t)=\frac{N_{e0}}{\tau\sqrt{\pi}}e^{-(\frac{t-3\tau}{\tau})^2}, \tag{9}$$

where τ is the time width of the pulse and and N_{e0} is the total number of electrons per unit area to be released during the duration of the pulse. We assume that secondary ion emission due to electron impact at the anode is negligible, so that the inward fluxes of ions at the cathode and anode and electrons at the anode are zero:

$$\Gamma_+^{in}(x=d)=\Gamma_+^{in}(x=0)=\Gamma_e^{in}(x=d)=0. \tag{10}$$

We use the classical form for Townsend's first coefficient:[11]

$$\alpha(|E|)=Ape^{-Bp/|E|}, \tag{11}$$

where A and B are empirically determined, gas-dependent coefficients, p is the neutral pressure and E is the local electric field.

1. Non-Dimensionalization

We normalize each variable, q, to a reference variable, q', to form a non-dimensional parameter, $\overline{q}$, such that

$$\overline{q}\equiv\frac{q}{q'}. \tag{12}$$

The relevant variables and their normalizations are listed in Table 1.

The dimensionless governing equations are:

$$\frac{d\bar{n}_e}{d\bar{t}} = \bar{\alpha}\bar{n}_e\bar{E}-\frac{d}{d\bar{x}}\bar{n}_e\bar{E} \tag{13}$$

$$\frac{d\bar{n}_+}{d\bar{t}} = \bar{\alpha}\bar{n}_e\bar{E}+\frac{d}{d\bar{x}}\bar{n}_+\bar{\mu}_+\bar{E} \tag{14}$$

$$\frac{d^2\bar{\phi}}{d\bar{x}^2} = -\bar{N}_{e0}(\bar{n}_+-\bar{n}_e) \tag{15}$$

$$\bar{E} = -\frac{d\bar{\phi}}{d\bar{x}}$$

$$\bar{\alpha} = \exp\left[\bar{p}(1-1/\bar{E})\right]. \tag{16}$$

The boundary conditions (Equations 6-10) become:

$$\bar{\phi}(0,\bar{t}) = 0 \tag{17}$$

Dimensional Quantity q	Description	Reference Quantity q'
α	ionization coefficient	$\alpha' = \alpha_0 = Ape^{-\frac{Bpd}{V}}$
x	position coordinate	$x' = \frac{1}{\alpha_0}$
d	gap width	x'
E	electric field	$E' = V/d$
$\mu_{e,+}$	mobility	μ_e
$v_{e,+}$	velocity	$v' = \mu_e \frac{V}{d}$
t	time	$t' = x'/v'$
τ	temporal pulse width	t'
$n_{e,+}$	particle density	$n' = \alpha_0 N_{e0}$
p	neutral pressure	$p' = \frac{V}{Bd}$
N_{e0}	electron pulse density	$N' = \frac{V\epsilon_0}{ed}$
ϕ	electrostatic potential	$\phi' = \frac{V}{\alpha_0 d}$
$\Gamma_{e,+}$	particle flux	$\Gamma' = n'v'$

Table 1. Dimensional variables and reference quantities used in the calculation.

$$\bar{\phi}(\bar{d}, \bar{t}) = \bar{d} \tag{18}$$

$$\bar{\Gamma}_e(0, t) = \gamma\bar{\Gamma}_+(0, \bar{t}) + \frac{\bar{N}_{e0}}{\bar{\tau}\sqrt{\pi}} e^{-(\frac{\bar{t}-3\bar{\tau}}{\bar{\tau}})^2}. \tag{19}$$

Taking into account the possibility of a non-uniform electric field, we write Townsend's well-known breakdown criterion as:

$$\mu = \gamma \left\{ \exp[\int_0^d \alpha(x)dx] - 1 \right\} \geq 1. \tag{20}$$

In undervoltage breakdown, we choose $\mu < 1$ as an initial condition. Since we neglect the dependence of γ on electric field, we can interpret the phenomenon as an increase in μ resulting from an increase in $\int_0^d \alpha(x)dx$ (though we will see that that raising μ above unity is a necessary but not sufficient criteria for breakdown.)

The temporal pulse width should have no effect as long as it is much less than the electron transit time. In addition, we assume that $\bar{\mu}_+ = \mu_+/\mu_e$ is constant, an assertion that is true if both mobilities have the same pressure scaling and are independent of electric field ($\bar{\mu}_+$, the mobility ratio, is not to be confused with μ, the Townsend breakdown parameter.) The problem is therefore uniquely specified with five dimensionless parameters:

$$\bar{N}_{e0} = \frac{N_{e0}ed}{\epsilon_0 V} \qquad \mu_0 = \gamma(e^{\alpha_0 d} - 1)$$

$$\gamma \qquad \bar{\mu}_+ = \frac{\mu_+}{\mu_e} \qquad \bar{p} = \frac{pBd}{V}$$

We thus aim to find, for a given μ_0, $\bar{p}$, γ, and $\bar{\mu}_+$, the minimum $\bar{N}_{e0}$ that will result in breakdown.

B. Solution and Results

1. Solution Method

We treat the problem on two timescales. Fine time steps are used during the transit of the first electron avalanche so that electron dynamics during the pulse injection can be accurately described. Coarser time steps are then used to describe ion dynamics during subsequent avalanches. Time steps are dynamically calculated to satisfy the CFL stability condition,[13]

$$\Delta \bar{t} = \frac{\Delta \bar{x}}{\max |\bar{v}|} \nu, \tag{21}$$

where ν, the Courant number, is held at a fixed value of .95. The relevant wave speed during the electron pulse transit is the electron drift velocity, but the ion drift velocity is used thereafter. On the ion timescale, we calculate the electron flux by replacing Equation 13 with the approximation:

$$\bar{\Gamma}_e(\bar{x}, \bar{t}) = \bar{\Gamma}_e(0, \bar{t}) \exp \int_0^{\bar{x}} \bar{\alpha}(\bar{x}, \bar{t}) d\bar{x}. \tag{22}$$

This approximation is valid provided that the electron flux from the cathode does not change significantly during an electron transit time, which is the case for most of the breakdown process, but that does not hold during the injection of the electron pulse.

We solve Equations 13 - 16 numerically using a 1D time-dependent finite-volume method.[13] Equations 13 and 14 are advection-reaction equations and are solved using an upwind scheme so that at the mth time step at position i,

$$n_i^m = n_i^{m-1} - \frac{v\Delta \bar{t}}{\Delta \bar{x}} (n_i^{m-1} - n_{i-1}^{m-1}) + \Delta \bar{t} \bar{\alpha}_i^{m-1} \bar{v}_e \bar{n}_e, \tag{23}$$

where n is either the non-dimensional ion or electron density and v is the relevant non-dimensional drift velocity.

Poisson's equation (15) is solved subject to the boundary conditions (17) and (18) at every time step using a tridiagonal inversion method.[14]

C. Theoretical Results

In Figure 5 we plot the normalized electron and ion densities and electric field during the first avalanche transit. Introduced at the cathode, the electron pulse drifts across the gap, grows due to ionizing collisions, then exits at the anode. The ions it created are left behind due to their lower mobility and the resulting charge imbalance distorts the electric field, enhancing it near the cathode but suppressing it near the anode. One can show[15] that $\int_0^d \alpha(x)dx$ will increase if $\bar{p}$ exceeds a critical value which ranges from approximately 1.6 to 2. If this is the case, ionization will be enhanced for subsequent avalanches and breakdown *may* occur.

For convenience, we introduce a dimensionless time parameter:

$$\xi \equiv \frac{t}{T_+ + T_e}, \tag{24}$$

where $T_{+,e} = d/(\mu_{+,e} E_0)$ are the transit times of the ions and electrons as a result of the unperturbed field. In the absence of space charge effects, 1 ξ would be the duration of one avalanche generation.

We plot the normalized ion density distribution as a function of ξ for two cases: in Figure 6 an injected electron pulse that is not large enough to cause breakdown and in Figure 7 a larger pulse which does cause breakdown. The first electron avalanche appears instantaneous on this time scale, so the initial condition is the ion distribution resulting from that avalanche. The ions drift toward the cathode ($\bar{x} = 0$), releasing second-generation electrons due to secondary emission. Those electrons instantaneously result in second-generation ions, which in turn drift toward the cathode, producing further avalanche generations. Since $\mu < 1$ is always an initial condition, we expect each generation to be smaller than the previous in the absence of space charge distortion. In the first case (Figure 6), this behavior is evident, as successive avalanches gradually die out in magnitude. In the second case (Figure 7), however, the space charge distortion is large enough to reverse that trend; the avalanches increase in size and quickly merge, which will result in breakdown.

The key to achieving breakdown is the ability to raise μ above unity through an increase in $\int_0^d \alpha(x)dx$. In Figure 8 we plot μ vs ξ for various injected pulse densities. In each case, μ's initial value, μ_0, is .85, but is instantaneously increased as a result of the initial electron avalanche. As successive avalanches develop, μ rises and falls with the redistribution of ion density.

In all cases, μ is made to exceed unity at least temporarily. However, in some cases, μ falls below it again and a breakdown is not achieved. Furthermore, there are cases in which μ exceeds unity, then drops

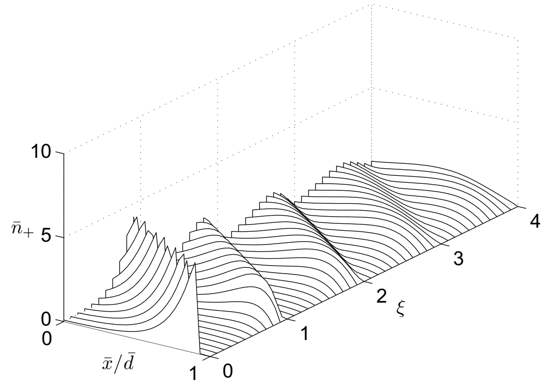

Figure 6. Normalized ion density distribution as a function of ξ for $\bar{p} = 2.15, \mu_0 = .95, \gamma = 7.13 \times 10^{-4}, \bar{\mu}_+ = .004$ and $\bar{N}_{e0} = 5 \times 10^{-3}$. The avalanche generations gradually die out and no breakdown will occur.

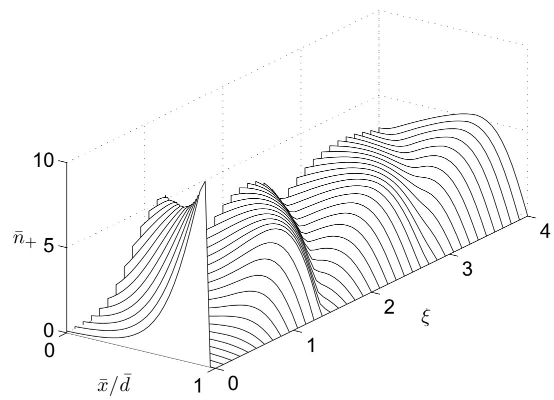

Figure 7. Normalized ion density distribution as a function of ξ for $\bar{p} = 2.15, \mu_0 = .95, \gamma = 7.13 \times 10^{-4}, \bar{\mu}_+ = .004$ and $\bar{N}_{e0} = 1.5 \times 10^{-2}$. Here the avalanches build in magnitude; a breakdown will eventually result.

below it, then increases again resulting in breakdown. It is therefore clear that Townsend's classic breakdown condition, $\mu > 1$, does not apply for undervoltage breakdown.

The Townsend model requires positive gain over several avalanche generations in order for breakdown to be achieved. μ is intended to be the ratio of the number of electron-ion pairs in one generation to the previous one. However, the quantity μ varies *during* each ion avalanche transit. It is not surprising, then, that one can instantaneously achieve $\mu > 1$, temporarily producing a lot of next-generation electrons, but not sustain that state for the entire ion transit. In such a case, the total number of charge carriers produced in the next generation might not be greater, and breakdown would not be achieved. Still, it seems obvious that if μ never exceeds unity, a breakdown will never occur. We can thus say that $\mu(t) > 1$ is a necessary but not sufficient condition for undervoltage breakdown.

Such examination of the development of μ allows us to address the question of threshold criteria. We designate an event as a breakdown if μ trends upward over several ξ, then use the method of bisection to find the minimum $\bar{N}_{e0}$, a parameter we define as $\bar{N}_{e0}^*$, that will result in breakdown as a function of the other four input parameters.

Figures 9-11 contain threshold curves, plots of $\bar{N}_{e0}^*$ as a function of μ_0 for various values of $\bar{p}$, γ, and $\bar{\mu}_+$.

IV. Discussion

In Figure 12, we plot $\bar{N}_{e0}^*$ as calculated from the experimentally measured threshold charge values displayed in Figure 4. For each data point, we also plot the theoretically calculated value using published values

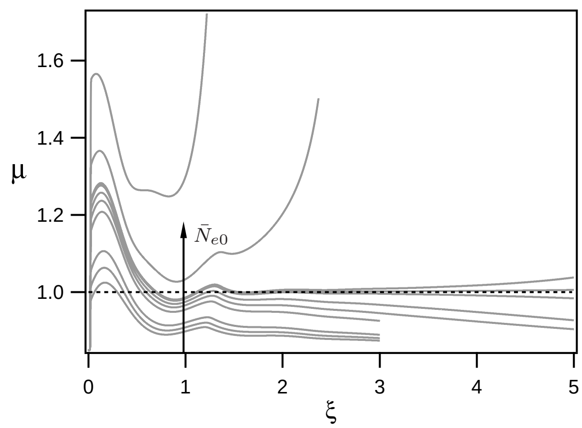

Figure 8. The temporal development of μ for various injected pulse sizes.

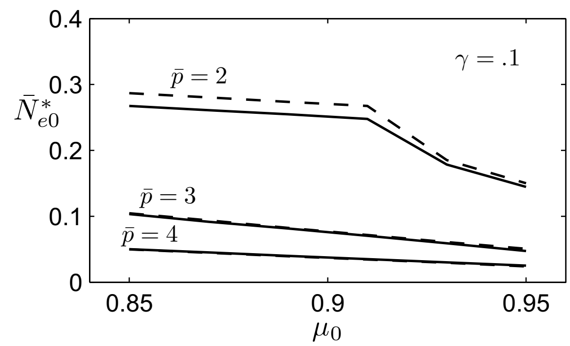

Figure 9. Threshold curves for γ=.1, $\bar{\mu}_{+}$=.004 (solid) and $\bar{\mu}_{+}$=.01 (dashed)

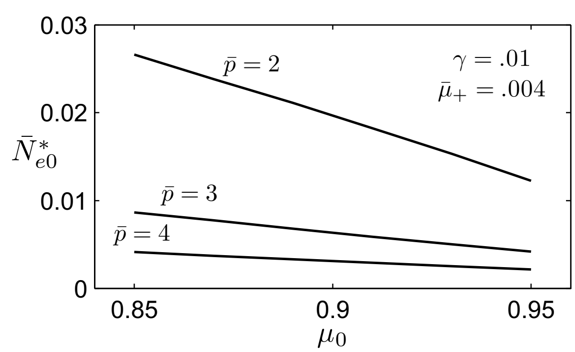

Figure 10. Threshold curves for $\bar{\mu}_{+}$=.004 and γ=.01.

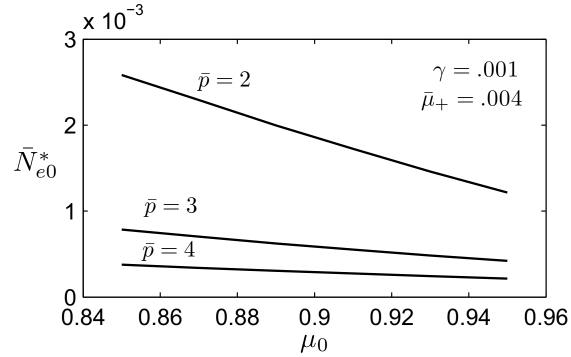

Figure 11. Threshold curves for $\bar{\mu}_+$=.004 and γ=.001.

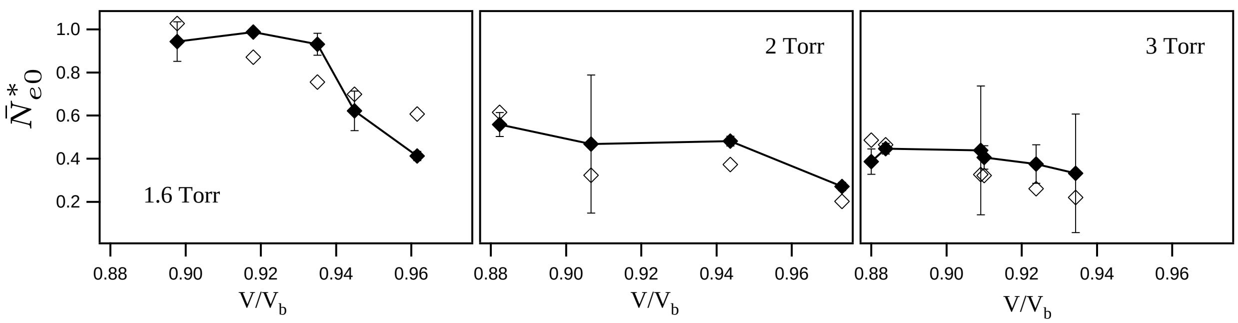

Figure 12. $\bar{N}^*_{e0}$ as measured (solid) and calculated for $\gamma = .1$ (open).

for the Townsend ionization coefficients[11] for argon and assuming $\gamma = 0.1$. The true secondary emission coefficient, and its dependencies on electric field and pressure, are highly dependent on surface conditions[16] and are not well known. That value of γ was chosen because it generates good agreement between predictions and data, but it happens to fall within an expected range for these experimental conditions.

The dimensionless parameter $\bar{N}^*_{e0}$ represents the ratio of the critical injected charge to the charge on the electrodes and ranges within values on the order of 10^{-1} for these experimental conditions. In order to enhance ionization through a distortion of the applied electric field, we must provide sufficient charge to compete with that field. Ionization will amplify the injected charge, but at low gain, the initial charge must still be significant fraction of the applied charge. This is the fundamental difference between the phenomenon we are investigating, undervoltage breakdown through the Townsend mechanism at low gain, and breakdown in higher-gain devices, in which a single electron can start an avalanche that forms a streamer.

The trend of decreasing $\bar{N}^*_{e0}$ with increasing pressure ($\bar{p}$) is a demonstration of the importance of the α-process to undervoltage breakdown. At higher pressure, ionization is more field-limited than pressure-limited, and the system is more sensitive to increases in electric field such as those caused by the space charge distortion.

The relevance of the α process to undervoltage breakdown also explains the theoretically predicted dependence of critical pulse size on the secondary emission coefficient. Increasing γ increases $\bar{N}^*_{e0}$ because, at constant μ_0, higher γ implies lower $\alpha_0 d$. Since undervoltage Townsend breakdown is achieved through manipulation of gas amplification and not secondary emission, the phenomenon is more difficult to achieve when the amplification factor is reduced.

The weak dependence on ion mobility (Figure 9) suggests that breakdown is determined during the first electron avalanche. The charge imbalance produced when the electrons leave the volume represents the largest electric field distortion that will occur during the breakdown process, raising μ above unity and increasing ionization for subsequent avalanches. However, on the timescale of an electron avalanche, even the lightest ions are essentially stationary, and the mobility ratio is not relevant. Ionization increases and decreases in a complex fashion as further avalanches develop, but the general trend of growth or damping is established very early. The ion dynamics have only a minor effect on this process.

Using published data on the Townsend coefficients for Argon,[11] we can calculate that $\bar{p} = 2$, for the voltage range used in these experiments, corresponds to pressures ranging from 1.3 Torr to 1.6 Torr at these voltages. The theoretical predictions of[15] suggest that these represent approximate critical pressures below which undervoltage breakdown should not be possible, and indeed, no breakdowns were observed below 1.6 Torr.

V. Conclusions

We have experimentally and theoretically explored threshold conditions for undervoltage breakdown, the conditions under which a pulse of electrons will induce breakdown through the Townsend mechanism in a low-gain ($\exp(\alpha d) < 10^4$) discharge gap that is held below its breakdown voltage. From this investigation, we have gleaned the following physical insights into the phenomenon:

- $\mu > 1$ is necessary for undervoltage breakdown, but not sufficient.
- To achieve breakdown at low gain, the space charge distortion must result from the magnitude of the injected pulse, so the injected charge must be significant when compared with the charge on the electrodes.
- Undervoltage breakdown is controlled by electron-impact ionization. It is thus easier as gain is increased, or as that process' sensitivity to electric field distortion is increased, such as through increases in pressure.
- Whether or not breakdown will occur is decided during, and immediately after, the transit of the first electron avalanche that results from the injected pulse. The phenomenon is therefore insensitive to ion mobility.

VI. Acknowledgements

The authors are thankful for support from the Program in Plasma Science and Technology at the Princeton Plasma Physics Laboratory.

References

[1] Cooley, J. and Choueiri, E., "Fundamentals of PPT Discharge Initiation: Undervoltage Breakdown Through Electron Pulse Injection," 39^{th} *Joint Propulsion Conference*, Huntsville, AL, 2003, AIAA-2003-5027.

[2] Berkery, J. and Choueiri, E., "Laser Discharge Initiation for Gas-fed Pulsed Plasma Thrusters," 37^{th} *Joint Propulsion Conference*, Salt Lake City, UT, 2001, AIAA-2001-3897.

[3] Cooley, J. and Choueiri, E., "Fundamentals of Discharge Initiation in Gas-Fed Pulsed Plasma Thrusters," 29^{th} *International Electric Propulsion Conference*, Princeton, New Jersey, September 2005, IEPC 2005-153.

[4] Kluckow, R., "ber den zeitlichen Verlauf des Stromes einer Gasentladung in Wasserstoff," *Z. Phys. A*, Vol. 161, No. 4, Aug 1961.

[5] Raether, H., *Electron Avalanches and Breakdown in Gases*, Washington, Butterworth Co, 1964.

[6] Frechette, M., Bouchelouh, N., and Larocque, R., "Laser-Induced Undervoltage Breakdown in Atmospheric N_2 Correlated with Time-Resolved Avalanches," *IEEE International Sumposium on Electrical Insulation*, Pittsburgh, PA, June 5-8 1994.

[7] Sato, N. and Sakamoto, S., "Undervoltage breakdown between parallel plates in air," *J. Phys. D: Appl:Phys*, Vol. **12**, 1979, pp. 875–886.

[8] Fonte, P., "A Model of Breakdown in Parallel-Plate Detectors," *IEEE Transactions on Nuclear Science*, Vol. **43**, No. 3, June 1996, pp. 2135.

[9] Fonte, P., Peskov, V., and Sauli, F., "Feedback and breakdown in parallel-plate chambers," *Nuclear Instruments and Methods in Physics Research A*, Vol. **305**, 1991, pp. 91.

[10] Engel, A. V. and Steenbeck, M., *Elektrische Gasentladungen*, Verlag Von Julius Springer, 1932.

[11] Raizer, Y., *Gas Discharge Physics*, Springer-Verlag, 1997.

[12] Šijačić, D. and Ebert, U., "Transition from Townsend to glow discharge: Subcritical, mixed, or supercritical characteristics," *Physical Review E*, Vol. **66**, 2002, pp. 066410.

[13] Leveque, R., *Finite Volume Methods for Hyperbolic Problems*, Cambridge University Press, 2002.

[14] Press, W., Teukolsk, S., Vetterling, W., and Flannery, B., *Numerical Methods in C*, Cambridge University Press, 2002.

[15] Cooley, J. and Choueiri, E., "A Universal Scaling Parameter for Undervoltage Breakdown," *submitted for publication.*

[16] Phelps, A. and Petrovic., Z. L., "Cold-cathode discharges and breakdown in argon: surface and gas phase production of secondary electrons," *Plasma Sources Sci. Technol*, Vol. **8**, No. R21, 1999.